ELSEVIER

Polymer 44 (2003) 3001–3008

polymer

www.elsevier.com/locate/polymer

In situ synchrotron study of the solution crystallization of ultralong alkanes from dilute solution

A.E. Terry[a], J.K. Hobbs[b], S.J. Organ[c], P.J. Barham[b,*]

[a]*Department of Zoology, University of Oxford, South Parks Road, Oxford OX1 3PS, UK*
[b]*H H Wills Physics Laboratory, University of Bristol, Tyndall Avenue, Bristol BS8 1TL, UK*
[c]*Department of Materials Engineering, The Open University, Walton Hall, Milton Keynes MK7 6AA, UK*

Received 20 November 2002; received in revised form 20 February 2003; accepted 21 February 2003

Abstract

The crystallization from dilute solution of two long *n*-alkanes ($C_{246}H_{494}$ and $C_{162}H_{326}$) has been followed in real time using synchrotron X-ray diffraction techniques at the European Synchrotron Radiation Source (ESRF) at Grenoble.

The data confirm the existence of minima in crystallization and nucleation rates in $C_{294}H_{590}$. Further, the ability to record data very rapidly has allowed us to see the minimum in crystallization rate in $C_{162}H_{326}$ for the first time.

Small changes in lattice spacing were seen during and after crystallization in all samples. These indicate that there is some perfectioning of crystals—for example the removal of cilia at the surfaces, etc.

Keywords: Crystallization; *n*-Alkane; Crystallization rate minimum polymer crystallization

1. Introduction

Monodisperse long *n*-alkanes with chain lengths spanning the range between extended chain and chain-folded crystallization have proved valuable model materials for studying many aspects of polymer crystallization [1,2]. A recent review provides a comprehensive summary of the key results obtained using these and other model compounds [3]. Of particular relevance to this paper are studies involving crystallization of alkanes from dilute solution, where a strong preference has been found for crystals to grow with thicknesses which are close to exact integer fractions (IF) of the extended chain length [2,4].

Crystallization kinetics have been followed previously in solution using a well-established DSC technique and have revealed pronounced minima in both nucleation and growth rate over the temperature range where the initial crystallization changes from one folded chain conformation to another. These minima have been observed in $C_{198}H_{398}$ and $C_{246}H_{494}$ for the transition between extended chains and once folded chains and in $C_{246}H_{494}$ and $C_{294}H_{590}$ for the transition between once folded chains and twice folded chains [5–8]. Previously unpublished data showing the variation in transition temperature with solution concentration in $C_{294}H_{590}$ are included here and are used as a temperature calibration for the current experiments. The DSC technique used relied on measurements of dissolution peak area as a function of crystallization time, as described in Ref. [6]. Different crystal types are clearly distinguishable by their widely separated dissolution temperatures: both initial crystallization and, in some cases, subsequent crystal thickening can be followed. The validity of this method has been questioned by some authors [9,10] who did not observe growth rate minima in similar materials obtained by a different method [11] and who claimed that the minima may be an artefact arising from a combination of primary growth and subsequent re-organization. The synchrotron experiments described here have enabled us conclusively to confirm previous observations of growth and nucleation rate minima during crystallization of $C_{294}H_{590}$ from dilute solution, by directly following the development of crystalline material over time from the X-ray diffraction patterns. In addition we report the first growth rate measurements from $C_{162}H_{326}$ crystallized from solution.

* Corresponding author. Tel.: +44-117-9288711; fax: +44-117-9255624.
E-mail address: peter.barham@bristol.ac.uk (P.J. Barham).

0032-3861/03/$ - see front matter © 2003 Elsevier Science Ltd. All rights reserved.
doi:10.1016/S0032-3861(03)00211-8

Rate inversions have also been identified during melt crystallization of *n*-alkanes by direct observation of crystal growth in $C_{246}H_{494}$ [12] and from DSC measurements of six different alkanes in the range $C_{194}H_{390}$–$C_{294}H_{590}$ [13,14]. Synchrotron studies of melt crystallization of $C_{246}H_{494}$ [15] have revealed the presence of non-integer folded (NIF) crystal forms with a more disordered surface layer during the early stages of melt crystallization, which subsequently transform by thickening or thinning into the more stable IF forms. There is evidence to suggest that this disordered layer contains long uncrystallized chain ends (cilia) from molecules which have 'half-crystallized' and which are subsequently drawn into the crystals by a process of chain translation [16,17]. The ability of the chains to reorganize during growth implies a high degree of chain mobility within the crystal lattice, which has also been observed during recent studies of morphological changes that occur during crystal thickening [18].

The minima in growth and nucleation rates, which occur in the temperature range where crystallization changes from one stable crystal form to another, have been attributed to a 'poisoning' effect at the crystal growth face. It has been proposed that the growth of potentially stable (less folded) chains is blocked by the temporary deposition of unstable (more folded) chains on the growing face of the crystal [15]. According to this model the residence time of the unviable chain conformations increases as the temperature is decreased, until a point is reached where the more folded chains become stable and crystals can grow freely in this form. Simple rate equation models and computer simulations based on this hypothesis have proved successful in modeling the general behavior [19]. An alternative explanation based on secondary nucleation theory has also been proposed [20].

The current work extends the use of synchrotron radiation to study in situ crystal growth from dilute solution. We believe that this represents the first attempt to use X-rays to monitor synthetic polymer crystallization from dilute solution. We have been able to detect crystallinity at concentrations as low as 0.1%, allowing meaningful rate data to be obtained from a 0.7% (w/w) solution. Data has been obtained for $C_{162}H_{326}$ for the first time, since the crystallization and transformation rates had proved too rapid to be studied by other means. The existence of the minimum in crystal growth rate in $C_{294}H_{590}$ has been convincingly confirmed. At each crystallization temperature it was possible to monitor the variation in *d*-spacing of the principal reflections both during initial crystallization and on subsequent annealing. Subtle changes in crystal lattice spacing over time have been identified which are not associated with crystal thickening. A gradual contraction of the crystal lattice after primary crystallization is complete has been observed which is contrary to the expectation that crystals grown under these conditions (relatively slow growth rates, from chains that are uniform in length and short in polymeric terms) would be essentially perfect. The implied slow increase in order over time is discussed in relation to some recently proposed models of polymer crystallization.

2. Experimental details

Samples were prepared from the *n*-alkanes $C_{162}H_{326}$ and $C_{294}H_{590}$ kindly provided by Brooke [21] and the Engineering and Physical Sciences Research Council of the UK (EPSRC).

A measured amount of alkane (typically 0.1–0.5 mg) was placed in a 2 mm-diameter Lindemann tube and sufficient toluene was added to give a concentration of approximately 1, 3 or 5%. The Lindemann tubes were then shortened and flame sealed to prevent evaporation of solvent during the experiment. For exposure to the X-ray beam the samples were mounted in a modified silver block Linkam hotstage, with the tube at an angle of about 45° to the horizontal. The sample was positioned such that the X-ray beam passed through the tube a few millimetres from its end and adjusted so that the solvent scatter was at a maximum (i.e. through the thickest available section of the tube). A metal cover was used to hold the samples against the silver block; this ensured good thermal contact and allowed accurate positioning of the Lindemann tubes after changing the samples. The temperature of the silver block was recorded using the internal platinum resistor and the temperature at the start of collecting a diffraction pattern was recorded alongside the pattern.

The wide-angle diffraction data were collected at the Materials Science beamline, ID11, at the ESRF. The X-ray wavelength was 0.5166 Å and the beam size was 300 μm × 300 μm. Each two-dimensional diffraction pattern was collected for 3 s using a Bruker Smart CCD, which in its high resolution mode has a sensitive area of $16 \times 16\ mm^2$ consisting of 2000×2000 pixels each of size 78 μm × 78 μm. The read-out time is necessarily slow and total deadtime between images was 12 s. The sample–detector distance was 0.2 m and was calibrated using a silicon standard. The resulting two-dimensional data were corrected for spatial distortions prior to integration. After subtraction of the solvent background a psuedo-Voigt function was fitted to the one-dimensional integrated data to produce values for the peak positions, full-width-half-maximum and total intensity.

Each sample was first heated to dissolve the alkane, as evidenced by the disappearance of the diffraction pattern. The resultant solution was then cooled at 20 °C min^{-1} until the desired crystallization temperature, T_c, was reached, then held isothermally for some time t_c. Crystallization temperatures were chosen to cover the range where, from previous experience, a change was expected to occur between two different forms of primary crystallization. For $C_{294}H_{590}$ the range of crystallization temperatures used was 83–89 °C: other experiments [7] have identified that

crystals grow from dilute solution with chains folded twice at the lower end of this range, while crystals grown at the higher temperatures contain chains folded only once. For $C_{162}H_{326}$ we can use the crystallization temperature at which a dissolution peak corresponding to once-folded chain crystals first appears as an approximation to the transition temperature from extended chain to folded chain growth. This identifies the temperature range of interest to be between 70 and 80 °C. The range of accessible temperatures was severely limited by the thermal lag of the apparatus for this fast growing alkane.

X-ray diffraction patterns were collected every 15 s, with an exposure time of 3 s, as described above. The beam was turned off between exposures. The onset of crystallization could be clearly seen from the initial appearance of the diffraction pattern. In most cases, crystallization was allowed to proceed until a maximum intensity appeared to have been reached. In a few cases much longer t_cs were used so that any changes in *d*-spacing or intensity which occurred after the initial crystallization could be observed.

3. Results: general comments

The results presented below were obtained from two samples for which extensive data sets were collected, and are typical of the general behavior. There were problems with some samples due to leakage of solvent, but this was easily identified and the results rejected. Successful samples were used many times; crosslinking eventually became apparent from an increase in dissolution temperature and no further measurements were then made.

Collection of diffraction data commenced before the sample reached the crystallization temperature to ensure that no detectable crystallization occurred during cooling: however, the results are displayed such that time $t_c = 0$ corresponds to the time at which the sample reached T_c. Crystallization is judged to have started as soon as a peak can be resolved above the noise. The rate of crystallization is measured from the slope of the linear portion of the intensity vs. time graph for the (110) reflection. Final values of intensity vary for the same sample at different crystallization temperatures and tended to be lower near the minimum in crystallization rate. Small variations may be due to an uneven distribution of material throughout the sample, or may be an indication that not all samples have completely crystallized during the experiment. Values are therefore given for both rate (using absolute values of intensity) and normalized rate (assuming the final value to correspond to 100% crystallization) in each case.

Modifications made to the Linkam hotstage introduced a small error into the temperature calibration of the instrument. A correction was applied using the previously unpublished DSC data from $C_{294}H_{590}$ given in Fig. 1, which shows the dependence of the transition temperature on concentration. The transition from once folded to twice

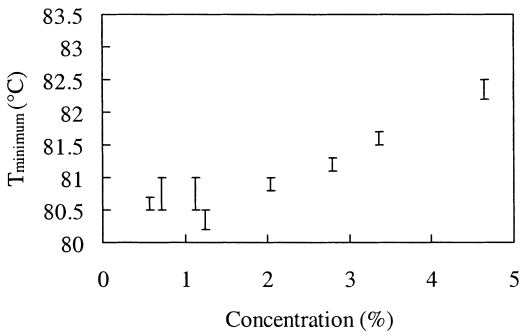

Fig. 1. Variation of transition temperature with concentration for $C_{294}H_{590}$ in toluene. $T_{minimum}$ is the temperature corresponding to the minimum in crystallization rate, where a transition occurs from growth of crystals containing once-folded chains (1F) to those containing twice-folded chains (2F). The error bars represent the gap between the highest temperature at which 2F crystals were detected and the lowest temperature at which only 1F crystals were obtained, as measured by DSC.

folded chains is known to correspond to the minimum in crystallization rate. For a 5% solution in toluene Fig. 1 shows a value of approximately 82.5 °C for this temperature, while the measured temperature of the minimum in growth rate for a similar sample in this experiment was 84.5 °C. A temperature correction of −2.0 °C has therefore been applied to all subsequent results: this temperature error is not unreasonable considering the large thermal mass of the tube holder. Uncertainties in the precise concentration of the samples and in the range covered by the 'error' bars in Fig. 1 produce an overall uncertainty in temperature calibration of ±0.5 °C.

3.1. Results: $C_{294}H_{590}$

The results presented here are from a 5% solution of $C_{294}H_{590}$ in toluene. This relatively high concentration gave particularly clear diffraction data over a wide range of crystallization temperature. A typical diffraction pattern is shown in Fig. 2(a). The characteristic 110 and 200 reflections from the alkane crystal lattice are clearly visible against the amorphous halo arising from the solvent. Fig. 2(b) shows an example of the peak fitting applied to the data.

Fig. 3 shows some examples of plots of intensity vs. time for the (100) and (200) reflections, at different crystallization temperatures. It is clear from Fig. 3 that there are variations in both (a) the time taken for crystallization to reach detectable levels and (b) the rate at which the intensity of the diffraction peaks increases, with T_c. Each of these parameters is likely to have a complex relationship with both nucleation and growth rates, with (a) more closely linked to nucleation and (b) to growth.

In Fig. 4 the time taken from reaching the crystallization temperature until crystallization is just detectable in this experimental set-up (which we call the incubation time) is plotted against crystallization temperature for both the (110) and (200) reflections. There is a general increase in

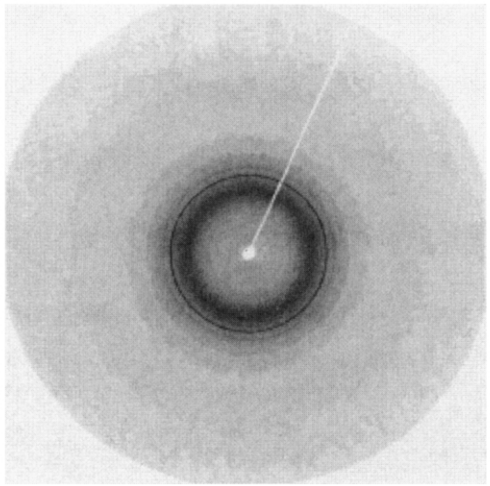

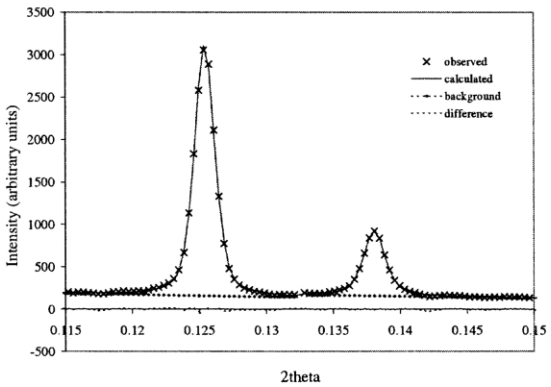

Fig. 2. Top, (a) typical diffraction pattern obtained from a 5% solution of $C_{294}H_{590}$ in toluene. The (110) and (200) reflections are clearly visible against the solvent background and faint higher orders are also present. Bottom, (b) an example of curve fitting to the (110) and (200) diffraction peaks, after subtraction of the solvent background.

incubation time with T_c, with the (110) reflection becoming visible slightly before the (200). However, the curve is not continuous. As the crystallization temperature is increased the incubation time reaches a peak at $T_c = 83.5$ °C, then drops down to lower values before eventually starting to rise again at $T_c = 85.0$ °C. The maximum in incubation time can be taken to imply a minimum in the number of active nuclei at this temperature.

Fig. 5 shows how the rate of increase in intensity of the X-ray reflections varies over the same temperature range. This provides a measure of the crystallization rate. In this case, we see a general decrease in crystallization rate with temperature, as expected, but can again identify discontinuities in the curve. A minimum in crystallization rate is observed at $T_c = 82.5$ °C, providing clear and convincing evidence for a rate inversion.

At a few temperatures samples were held isothermally in the X-ray beam for a considerable time after crystallization appeared to be complete. Two examples of the results obtained are shown in Figs. 6 and 7, for crystallization temperatures of 83.5 and 85.0 °C, respectively. Figs. 6(a), 7(a), and (c) show how the (110) d-spacing changes over time, while Figs. 6(b), 7(b), and (d) show the corresponding intensity data.

From Figs. 4 and 5 it can be seen that 83.5 °C is the temperature at which the maximum incubation time was observed, while 85 °C is well above the minimum in crystallization rate. In both cases we expect crystals to contain once-folded chains, but the onset of crystallization is delayed at 83.5 °C. In Figs. 6(a) and 7(a) the apparent initial rise in d-spacing is not reliable, since the amount of crystalline material at this stage is extremely small. However, the subsequent decrease in d-spacing seen in both cases is a genuine effect. In the sample held at 83.5 °C we see a very gradual decrease in d-spacing of approximately 0.3% over a time scale of 80 min. In the 85.0 °C sample the d-spacing starts from a higher initial value (as would be expected for a higher T_c) and follows a more complex curve: a relatively steep initial fall is followed by a much slower decrease akin to that seen at the lower temperature. A discontinuity is apparent in the steep portion of the curve.

The integrated intensity of the X-ray reflections first increases over time as the crystals grow, as shown in Figs. 6(b) and 7(b). This is the data from which the crystallization rate is calculated. It is interesting to note that the discontinuity noticed in the d-spacing after approximately 10 min growth at 85.0 °C is accompanied by a discontinuity in intensity. At both temperatures we observe a slight falling off in intensity as the sample is held at the crystallization temperature for an extended time. Similar, but less pronounced, changes are observed for the (200) reflections. The possible origin of these effects will be discussed below.

3.2. Results: $C_{162}H_{326}$

Crystallization proceeded much more rapidly in $C_{162}H_{326}$ than in $C_{294}H_{590}$, and this limited the range of temperatures that could be attained without crystallization occurring during cooling. The data presented here were obtained from a 0.7% (w/w) solution of $C_{162}H_{326}$ in toluene; for higher concentrations the crystallization rates were too high for the temperature range of interest to be accessible.

As before, plots of intensity as a function of time were obtained over a range of crystallization temperatures. From these measurements, values for the incubation time and the rate of increase in intensity were calculated at each temperature. The temperature calibration factor described above has been applied to all data.

Fig. 8 shows the incubation time (the time taken from reaching the crystallization temperature until crystallization starts) as a function of crystallization temperature.

The curve is very similar in form to that obtained from $C_{294}H_{590}$ and displays a clear maximum in incubation time, corresponding to a minimum in the number of active nuclei, at approximately 73.0 °C. The corresponding data for the rate of increase in intensity shown in Fig. 9 are much less

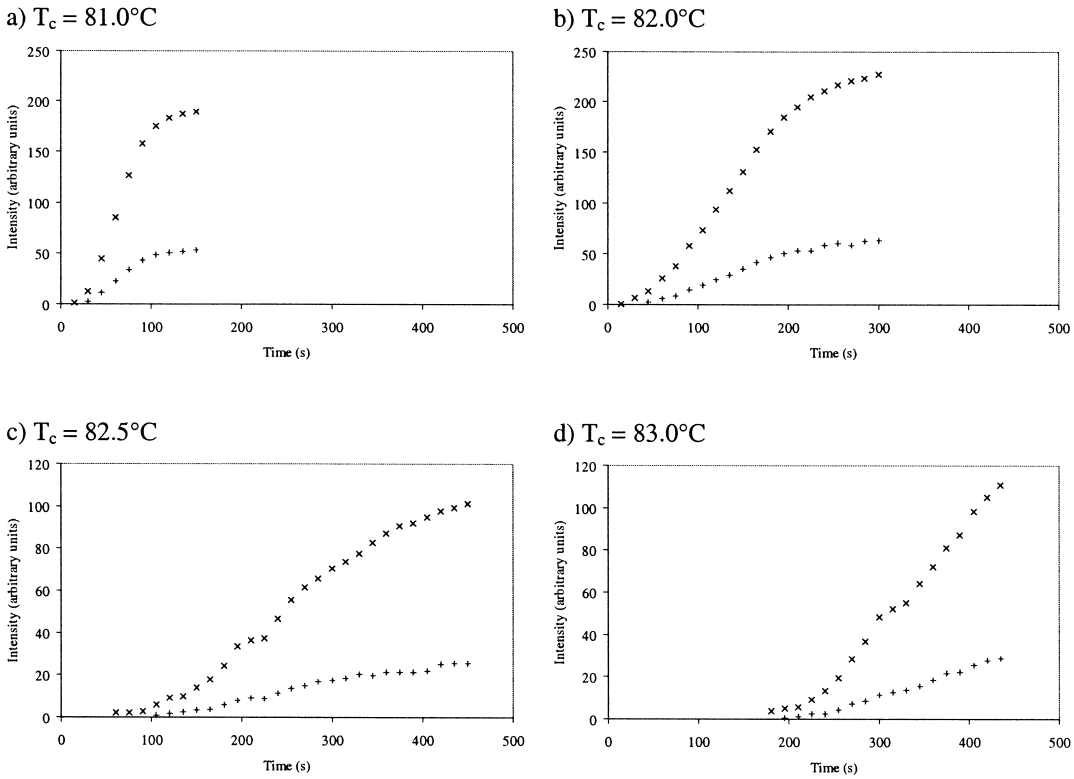

Fig. 3. Increase in intensity with time at crystallization temperatures in the range 81.0–83.0 °C for a 5% solution of $C_{294}H_{590}$ in toluene. The intensity is plotted in arbitrary units. (× (110) reflection + (200) reflection).

conclusive. No clear minimum in growth rate can be identified here.

Unsurprisingly, the data obtained from this very low concentration sample is of poorer quality than that shown previously for $C_{294}H_{590}$ but changes in *d*-spacing and intensity over time can nevertheless be identified. Downward steps in *d*-spacing accompanied by increases in intensity, similar to those observed in $C_{294}H_{590}$, were observed at several crystallization temperatures, both above and below the peak in incubation time. A typical example is shown in Fig. 10 for crystallization at 72 °C. No further decrease in *d*-spacing occurred in this sample after crystallization for 90 min either at this or at higher temperatures.

4. Discussion

This technique has proved successful for following crystallization in solutions with concentrations as low as 0.7%, representing cystallinity measurements lower than 0.1% during the early stages of growth. Samples could be used several times without any detectable deterioration resulting from exposure to the X-ray beam: indeed, due to the convective mixing of the sample, degradation rates due to beam damage are expected to be lower than in molten polymer samples. Crystal dissolution temperatures were checked at the start of every experiment and only showed changes after very long exposure times, after which samples were discarded. The modifications made to the Linkam

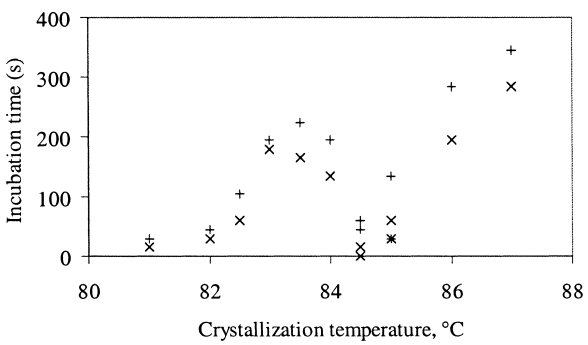

Fig. 4. Variation in incubation time with crystallization temperature for a 5% solution of $C_{294}H_{590}$ in toluene. (× appearance of (110) reflection + appearance of (200) reflection).

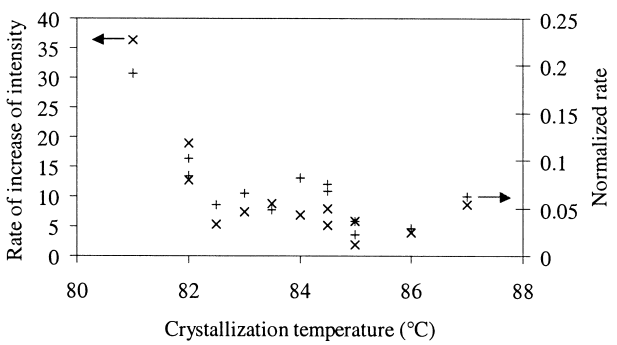

Fig. 5. Rate of increase in intensity of the (110) reflection as a function of time for a 5% solution of $C_{294}H_{590}$ in toluene. (× rate of increase in intensity (arb.units per second) + normalized rate).

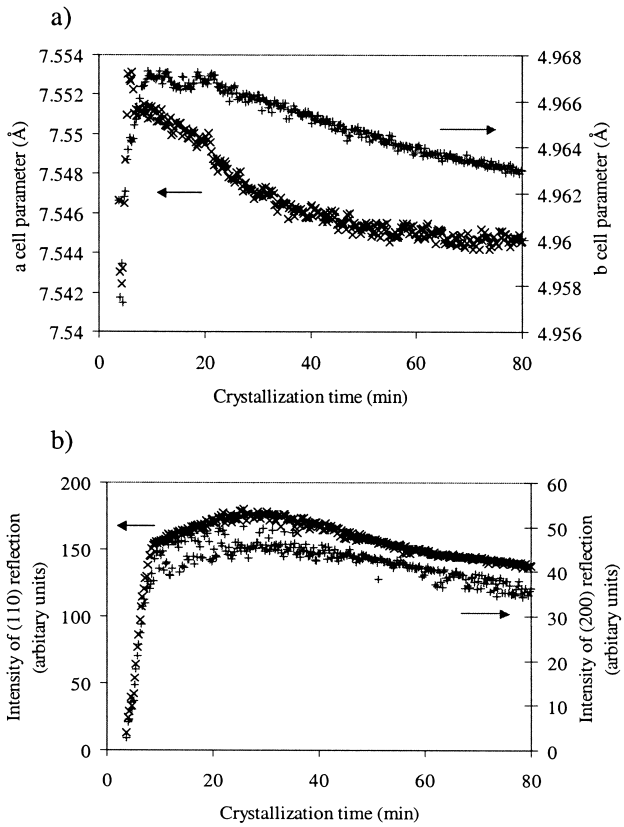

Fig. 6. Crystallization from a 5% solution of $C_{294}H_{590}$ in toluene at 83.5 °C. (a) shows how the *a* (×) and *b* (+) cell parameters vary with time, while (b) shows the change in intensity for the (110) (×) and (200) (+) reflections from which the cell parameters were calculated.

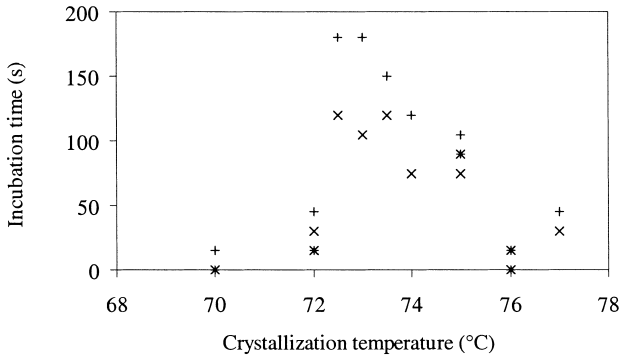

Fig. 8. Variation in incubation time with crystallization temperature for a 0.7% solution of $C_{162}H_{326}$ in toluene. (× appearance of (110) reflection + appearance of (200) reflection).

hotstage in order to support and locate the samples introduced a calibration error, for which we have corrected, and also some additional thermal lag in the system. This limited the range of crystallization temperatures accessible for the $C_{162}H_{326}$ samples. Results were examined to check for possible heating effects due to the X-ray beam, but since no evidence for thermal expansion of the crystal lattice was seen we can be confident that the crystallization occurred under isothermal conditions.

Temperature calibration was achieved through comparison of the position of the growth rate minimum in $C_{294}H_{590}$ with the results of DSC experiments that charted the variation in the position of the transition temperature with solution concentration.

This clear demonstration of a maximum in incubation time and a minimum in crystallization rate for $C_{294}H_{590}$ using a direct, and hitherto unproven, method confirms previous observations of rate minima in solution deduced

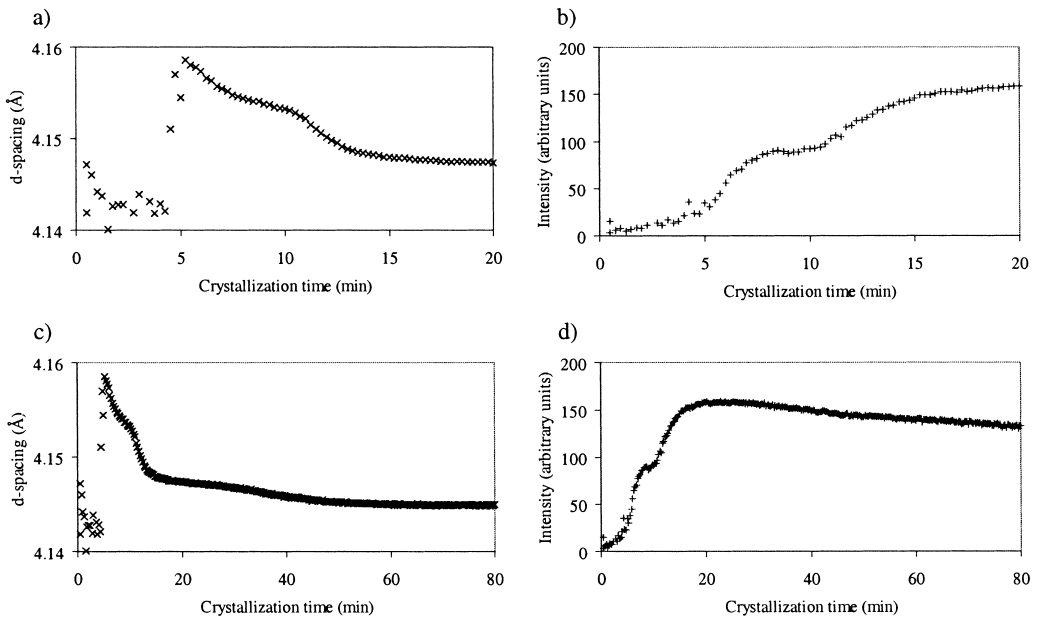

Fig. 7. Crystallization from a 5% solution of $C_{294}H_{590}$ in toluene at 85 °C. (a) shows how the *d*-spacing varies with time, while (b) shows the corresponding change in intensity. (c) and (d) show a longer term view.

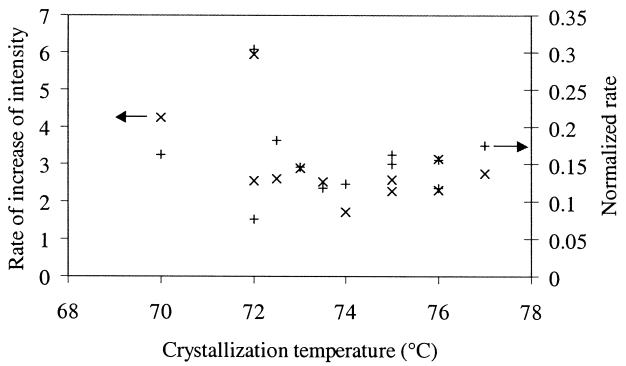

Fig. 9. Rate of increase in intensity of the (110) reflection as a function of time for a 0.7% solution of $C_{162}H_{326}$ in toluene. (× rate of increase in intensity (arb.units per second) + normalized rate).

from indirect DSC measurements. One advantage of the DSC method, however, is the possibility of identifying the different types of crystal from their dissolution temperatures. We have made no attempt in this work to identify different crystal forms independently, but have applied the results of previous studies in analysing our results. Thus we assumed that $C_{294}H_{590}$ crystals grown below the minimum in crystallization rate contain twice folded chains that will subsequently thicken into the once folded form, while those grown at higher temperatures contain once folded chains that do not thicken further. In similar work on melt crystallization [15,16] small angle X-ray measurements have been used to measure crystal thicknesses directly: such measurements are probably not feasible here due to the isolated nature of the single crystals in suspension.

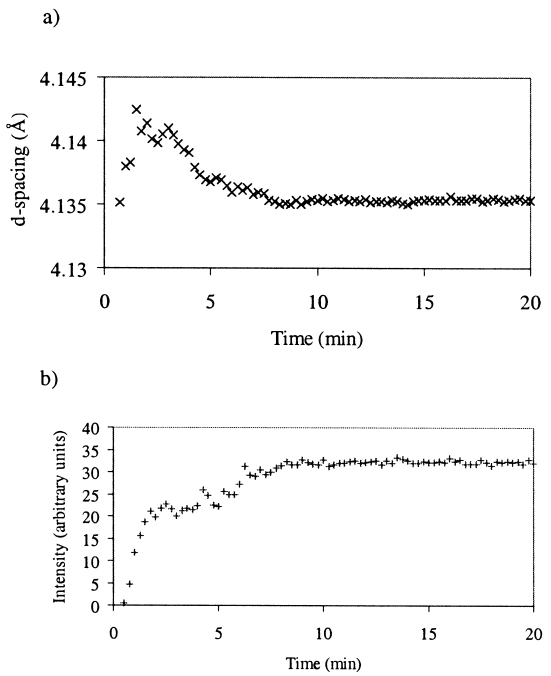

Fig. 10. Crystallization from a 0.7% solution of $C_{162}H_{326}$ in toluene at 72 °C. (a) shows how the *d*-spacing varies with time, while (b) shows the corresponding change in intensity.

No measurements have been obtained previously for the crystallization of $C_{162}H_{326}$ from dilute solution, as the growth rates are too fast to be followed by the DSC method. It is known that $C_{162}H_{326}$ can grow crystals containing chains that are either extended or folded once. It therefore seems reasonable to assume that the maximum incubation time observed here at 73.0 °C for a 0.7% solution of $C_{162}H_{326}$ in toluene is associated with that transition, with once folded crystals growing below 73 °C and extended chain crystals above 73 °C. The published data with which we can best draw a comparison is that for a 3.85% solution of $C_{198}H_{398}$ in toluene, where growth and nucleation rate minima were observed at 78 °C [5]. Since $C_{162}H_{326}$ is just a little shorter and since the solution concentration used here is lower, we would expect the transition in $C_{162}H_{326}$ to occur a few degrees below this. It is perhaps surprising that we do not see a minimum in the crystallization rate corresponding to the maximum incubation time. However, $C_{162}H_{326}$ is the shortest, fastest growing, of the alkanes to be studied. The higher mobility of the chain will permit rapid isothermal thickening, especially at temperatures just below the minimum in nucleation rate where folded chain crystals are only marginally more favored than extended chains. Seeding experiments using $C_{198}H_{398}$ have demonstrated that extended chain crystals will act as nuclei for further extended chain growth at temperatures just below the crystallization rate minimum, in preference to the folded chain crystals expected to grow in the absence of seeds [23]. If isothermal thickening takes place in $C_{162}H_{326}$ before primary growth is complete then the crystallization rate measured using this technique is likely to be higher than the true crystallization rate of folded chain crystal, as the measurement also includes fast growing extended chain crystals nucleated by thickened material. This is the most likely explanation for the absence of a clear minimum in crystallization rate for $C_{162}H_{326}$ (Fig. 9) despite the very obvious discontinuity in incubation time (Fig. 8).

Small changes in lattice spacing during or after primary crystallization were measured in both alkanes under some conditions. Of particular interest is the behavior shown in Fig. 7 for $C_{294}H_{590}$, where a pronounced decrease in *d*-spacing, accompanied by an increase in intensity, are observed simultaneously during the initial period of crystal growth, followed by a further more gradual decrease in lattice spacing over much longer crystallization times. These crystals are growing at a temperature where once folded chains are expected, and where isothermal thickening has never been observed in solution. The behavior seen here suggests that a considerable amount of re-organization is taking place after the initial stage of growth, as has been observed during melt crystallization [16]. One possible explanation for the discontinuity is that it corresponds to a pulling-in of initially uncrystallized cilia, allowing the lattice, originally strained by the dangling cilia, to contract and resulting in an increase in the total amount of crystallized material. Such an effect, which has been

recognized during melt crystallization, had not been expected from solution where the crystals grow more slowly than in the melt and the chains are less hampered by entanglements. The more gradual decrease in *d*-spacing over long periods of time is associated with a further slow perfectioning of the crystal lattice. This effect was quite general in $C_{294}H_{590}$, but was not observed in $C_{162}H_{326}$ where the more mobile chains are able to achieve a well ordered (extended chain) crystalline state with relative ease. The changes in lattice spacing in $C_{162}H_{326}$ may also include a component associated with chain unfolding. A recent synchrotron X-ray study of dried down crystals of several alkanes originally crystallized in chain folded forms [24] has clearly shown that a contraction in lattice parameter occurs when chains transform to a less folded form. In that case subtle changes in intensity and peak width were also detected which we have been unable to conclusively identify here due to the much lower quantity of crystalline material and the width of the tubes. However, decreases in lattice spacing were seen during the early stages of crystallization of $C_{162}H_{326}$ at temperatures both above and below the peak in incubation time so they cannot be exclusively attributed to crystal thickening.

The gradual decrease in intensity sometimes seen over long times is most likely due to a slow sedimentation of the crystals, reducing the amount of material in the path of the X-ray beam. Since we are dealing with a monodisperse system all the crystals should have identical chemical composition and hence we argue that any such sedimentation will only affect the overall intensity of the diffraction peaks and not their positions.

Possible models for explaining the minimum in crystal growth rate have been considered in detail elsewhere (for review, see Ref. [3]) and usually invoke a 'self-poisoning' effect where a growing crystal face is impeded by the temporary deposition of chains in a less favorable conformation. The changes in lattice spacing which occur on annealing at the crystallization temperature emphasize the non-equilibrium nature of the original crystallization process and also illustrate the tendency for changes to occur in a discontinuous manner. This is in accordance with recent simulations of crystal growth and annealing [25,26], which include the possibility of molecular reorganization behind the growth front. These simulations demonstrate the possibility of a series of intermediate crystalline states with different levels of internal energy and local order during the course of crystallization and subsequent annealing.

In summary, we have shown, for the first time, that direct measurements of crystallization rates for dilute solution of *n*-alkanes are possible. Further we have confirmed the existence of minima in crystallization and nucleation rates in $C_{294}H_{590}$. The intense X-ray source at the ESRF allows for more rapid data collection and has permitted us to make measurements in real time on $C_{162}H_{326}$ for the first time and to demonstrate on another system the minimum in crystallization rate.

References

[1] Bidd I, Holdup DW, Whiting MC. J Chem Soc, Perkin Trans 1 1987; 2455.
[2] Ungar G, Stejny J, Keller A, Bidd I, Whiting MC. Science 1985;299: 386.
[3] Ungar G, Zeng X. Chem Rev 2001;101:4157.
[4] Organ SJ, Keller A. J Polym Sci, Polym Phys Ed 1987;25:2409.
[5] Organ SJ, Ungar G, Keller A. Macromolecules 1989;22:1995.
[6] Organ SJ, Barham PJ, Hill MJ, Keller A, Morgan RL. J Polym Sci, Part B: Polym Phys 1997;35:1775.
[7] Morgan RL, Barham PJ, Hill MJ, Keller A, Organ SJ. J Macromol Sci-Phys 1998;B37(3):319.
[8] Hobbs JK, Hill MJ, Barham PJ. Polymer 2001;42:2167.
[9] Alamo R, Mandelkern L, Stock GM, Krohnke C, Wegner G. Macromolecules 1993;26:2743.
[10] Alamo R, Mandelkern L, Stock GM, Krohnke C, Wegner G. Macromolecules 1994;27:147.
[11] Lee KS, Wegner G. Makromol Chem, Rapid Commun 1985;6:203.
[12] Organ SJ, Keller A, Hikosaka M, Ungar G. Polymer 1996;37:2517.
[13] Boda E, Ungar G, Brooke GM, Burnett S, Mohammed S, Proctor D, Whiting MC. Macromolecules 1997;30:4674.
[14] Sutton SJ, Vaughan AS, Bassett DC. Polymer 1996;25:5735.
[15] Ungar G, Keller A. Polymer 1986;27:1835.
[16] Zeng X, Ungar G. Polymer 1998;39:4523.
[17] Ungar G, Zeng XB, Spells SJ. Polymer 2000;41:8775.
[18] Sanz N, Hobbs JK, Miles MJ. Manuscript in preparation.
[19] Higgs PG, Ungar G. J Chem Phys 1994;100:640.
[20] Hoffman JD. Polymer 1991;32:2828.
[21] Brooke GM, Burnett S, Mohammed S, Proctor D, Whiting MC. J Chem Soc, Perkin Trans 1 1996;1635.
[23] Ungar G, Organ SJ. J Polym Sci, Polym Phys Ed 1990;28:2353.
[24] Terry AE, Phillips TL, Hobbs JK. Macromolecules 2003; in press.
[25] Sommer J-U, Reiter G. Europhys Lett 2001;56(5):755.
[26] Welch P, Muthukumar M. Phys Rev Lett 2001;87(21):218302.